Discrete models of fabric accounting for yarn interactions

Simulations of uniaxial and biaxial behaviour

Bilel Ben Boubaker* — Bernard Haussy*
Jean-François Ganghoffer**

** ESEO, 4 rue Merlet de la Boulaye, F-49009 Angers cedex 01, BP 926*
Bernard.haussy@eseo.fr, Bilel.ben_boubaker@eseo.fr

*** LEMTA, UMR 7563, ENSEM, 2 Avenue de la Forêt de Haye*
B.P. 160, F-54504 Vandœuvre cedex
jfgangho@ensem.inpl-nancy.fr

ABSTRACT. *Discrete models of fabric have been elaborated at both macroscopic and mesoscopic scales, whereby nodes endowed with a mass and a rotational rigidity are mutually connected by extensible bars to form a two-dimensional trellis. At the macroscopic scale, the equilibrium shape of the structure is obtained as the minimum of its total potential energy versus the kinematic translational and rotational variables. Draping simulations are performed for fabric sheets lying on a fixed rigid surface. In the second part of the paper, a mesoscopic model of fabric is elaborated ; thereby, the undulations of the yarns are explicitly described within the unit cell, using a Fourier series development to represent the shape of each yarn. This methodology is applied to get the response of a set of intertwined yarns under biaxial loading, accounting for the contact reaction forces exerted by the transverse yarns.*

RESUME. *Des modèles discrets de structures tissées ont été élaborés aux échelles macroscopique et mésoscopique, considérant un réseau de nœuds dotés d'une masse et de rigidité en rotation, et connectés par des barres extensibles. L'ensemble de quatre barres délimitant un rectangle est doté d'une rigidité en torsion. La forme d'équilibre de la structure à l'échelle macroscopique est obtenue comme le minimum de son énergie potentielle, relativement aux variables cinématiques de translation et de rotation. Des simulations de drapé de nappes supportées par des formes rigides sont effectuées. Dans la seconde partie, on développe un modèle dit mésoscopique, qui prend en compte de façon explicite les ondulations des fils à l'intérieur de la cellule de base, la forme d 'équilibre des fils étant décrite par un développement en série de Fourier. Cette méthodologie est mise à profit pour évaluer la réponse d'une nappe de fils soumise à une sollicitation biaxiale, en tenant compte des efforts de réaction de contact des fils transverses.*

KEYWORDS: *woven structures, discrete models, draping simulations, stability analysis, mesoscopic approach, yarn-yarn interactions, uniaxial and biaxial loadings.*

MOTS-CLES : *structures tissées, modèles discrets, simulations du drapé, analyse de stabilité, approche mésoscopique, interactions entre fils, tractions uniaxiale et biaxiale.*

REEF – 14/2005. Composites forming simulation, pages 653 to 675

1. Introduction

The analysis of the deformations and shape forming of woven structures such as textiles is nowadays an important scientific and technological topic, due to the wide range of applications of these structures: mention *e.g.* mechanical parts made of dry fabric used in car and aerospace industry for their gain of weight ; apparel industry, or geotextiles. Since mechanical parts having complex shapes are produced on a large scale, it becomes important to have at hand tools for predicting the shape formability of fabric sheets. Although the mechanical properties and behavior of woven fabric reinforced composites has attracted many studies (Ishikawa *et al*., 1983), less work has been spent on dry fabrics (Kawabata, 1989), (Realf *et al*., 1993), (Gasser *et al*., 2000), (Boisse *et al*, 1997), (Boisse *et al*., 2001), (Magno *et al*., 2002), (Ganghoffer, 2003), despite their wide range of applications. The dry fabric behavior is quite peculiar, due to the ease of relative motions between yarns, which becomes prohibited when the initially dry fabric is impregnated with a resin: the lack of a matrix has thereby an important influence on the fabric behavior.

The mechanics of fiber fabrics is a three-scale imbricated problem, which calls for a micromechanical approach: at the microscopic scale, the basic constituents – the yarns – are made of single intertwined filaments, the organization of which may influence the contact and friction behavior during tension. At the intermediate scale, called the mesoscopic scale, the change of shape of the undulated yarns (warp and weft) and their extension lead to geometrical non-linearities. These deformation mechanisms and the arrangement of the yarns within the elementary woven pattern in turn determine the nonlinear complex behavior observed at the macroscopic scale. Considering this discrete constitution, it is relevant to analyze the behavior of the woven structure from the scale of a yarn or a set of intertwined yarns, possibly accounting for their mechanical coupling. The contact between the yarns, and their organization within the unit cell, that defines the type or armor (such as satin, serge) plays there an important role in the shape forming capacity of the initially flat structure (the pattern). It is therefore important to develop reliable and accurate micromechanical models, in order to be able to predict the 3D deformation of woven structures during real forming processes. These models can then further be used at the next scale (the macro scale) and implemented in FE codes (Realf *et al*., 1993), (Hing *et al*., 1996), (Bruckstein *et al*., 1990). This description can be refined, using the so-called meso-macro models that account for the nonlinearities due to the change of undulations of the yarns (Boisse *et al*., 2001), (Magno *et al*., 2002). A synthetic view of the modeling of woven structures is given in (Hing *et al*., 1996).

The goal of the present paper is accordingly to set up discrete models of fabric, involving beam like elements mutually connected to form a repetitive unit cell, that defines the basic fabric pattern. In connection to this, a given kinematics of the analogical elements (extensional, flexional and torsional springs) shall be elaborated. This kind of approach bears some resemblance with the work of (Provot, 1995), who models the tissue by a set of punctual masses connected with extensional, flexional

and shear-like springs. However, Provot model only considers the in-plane deformation of the pattern, and thus excludes the displacements of the nodes outside the initial plane of the tissue. This work is intended to give a synthetic review of the previous works published by the authors (Ben Boubaker *et al*., 2002; 2003).

The kinematic and static of the discrete model is first elaborated, thus leading to the expression of the total potential energy of, the unit cell. Draping simulations of fabric sheets on fixed rigid supports exemplify the potential of the model ; a stability analysis of a discrete fabric plate is conducted, using Dirichlet Lagrange stability criterion. In the second part of the paper, a mesoscopic refined analysis of the fabric is elaborated, which allows the consideration of the yarn undulations and yarn contact interactions within the unit cell. Simulations under biaxial loading are performed, and the impact of the transverse yarns properties on the yarn interactions is quantitatively assessed. Finally, some conclusions and perspectives are given.

2. Kinematics and sthenic of the discrete model. Energetic formulation

From a macroscopic point of view, the fabric is here considered as an orthotropic (at least in its initial reference configuration) elastic structure, the principal directions of which coincide with the warp and weft direction. The fabric sheet is modeled as a truss of elastic beams connected at frictionless hinges; the truss represents a mesoscopic view of the whole woven structure, that occupies a plane domain (x, y) in the initial stage, Figure 1a. The $z-$axis is selected in the direction normal to the plane (x, y). The nodes of the truss are labeled with two indices, the index i in the x direction, and the index j in the y direction. The elastic bars are represented by stretching springs of rigidity $C_{ex}^{i,j}$ (Figure1(c)). Rotational springs of rigidity $C_{b}^{i,j}$ are positioned at each grid node of mass $m_{i,j}$. It is assumed that such spring device at each node allows the rotations in the both directions (around the x and y axis) as shown in Figure1(e). To give the model a torsional rigidity, a spring device of rigidity $C_{t}^{i,j}$ is installed inside each set of four bars forming a rectangular chain (unit cell), Figure1(b). A shear spring of rigidity $C_{s}^{i,j}$ installed inside each basic cell, models the fabric shearing stiffness (Figure1(d)). The nodal kinematics variables attached to each node are the displacements $u_{i,j}$, $v_{i,j}$, $w_{i,j}$, and the rotation $\Psi_{i,j}$, as described in Figure1. The kinematics of the unit cell is associated to the following deformation modes:

– In-plane stretching (Figure 1c), described by two springs in the x and y directions;

– In-plane shear, represented by the diagonal springs in Figure 1d;

– Out of plane bending, due to the rotational spring on Figure 1e;

– Torsion, represented by the torsional spring on Figure 1b.

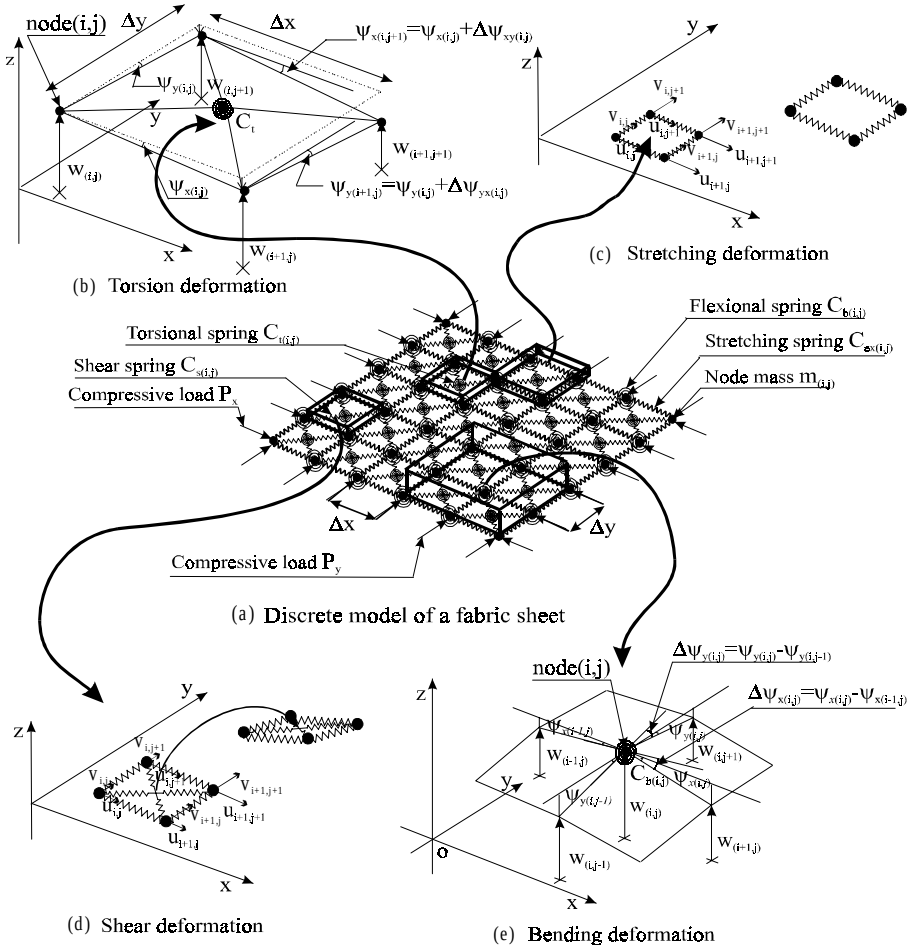

Figure 1a, b, c, d, e. *Kinematics of the macroscopic discrete fabric model*

Considering thin plates (only the case of monolayers of intertwined yarns shall be considered in the present study, with a small thickness to transversal length ratio), the kinematics and statics of the discrete model has been established in (Ben Boubaker *et al.*, 2002), whereby the discrete model mimics in an analogical manner an orthotropic thin plate structural model of the Kirchhoff type (Kikuchi *et al.*, 2000). Thereby, the mesoscopic behavior shall reflect the behavior being modeled and measured at the macroscopic scale, thus making the identification of the parameters easier.

The strain energy of the trellis U_s is obtained as the sum of the bending, torsional, stretching and shearing energy, deduced from the work of the internal

forces (moment resultants and force resultants) (Ben Boubaker, 2004). The extension energy, stored in the stretching spring $C_{ex}^{i,j}$, is expresses as:

$$U_{ex(i,j)} = \frac{1}{2} C_{ex}^{i,j} \left(\Delta u_{(i,j)}^2 \frac{\Delta y}{\Delta x} + \frac{E_2}{E_1} \Delta v_{(i,j)}^2 \frac{\Delta x}{\Delta y} + \left(\nu_2 + \frac{E_2}{E_1} \nu_1 \right) \Delta u_{(i,j)} \Delta v_{(i,j)} \right) \quad [1]$$

with $C_{ex}^{i,j} = \frac{hE_1}{1-\nu_1\nu_2}$ and E_1, E_2 the young modulus in the warp and weft directions respectively, G is the shear rigidity, and ν_1 and ν_2 are the Poisson's ratios in the warp and the weft directions. Δx and Δy are the finite difference grid lengths.

The shear energy, stored in the shearing spring $C_s^{i,j}$, is expressed as:

$$U_{sh(i,j)} = \frac{1}{2} C_s^{i,j} \left[\Delta u_{xy(i,j)}^2 \frac{\Delta x}{\Delta y} + \Delta v_{yx(i,j)}^2 \frac{\Delta y}{\Delta x} \right], \text{ where } C_s^{i,j} = Gh \quad [2]$$

with G the shear modulus.

The bending energy, associated with the flexional spring $C_b^{i,j}$, is obtained as:

$$U_{b(i,j)} = \frac{1}{2} C_b^{i,j} \left[\begin{array}{l} \Delta\psi_{x(i,j)}^2 \frac{\Delta y}{\Delta x} + \frac{E_2}{E_1} \Delta\psi_{y(i,j)}^2 \frac{\Delta x}{\Delta y} \\ + \left(\nu_2 + \frac{E_2}{E_1} \nu_1 \right) \Delta\psi_{x(i,j)} \Delta\psi_{y(i,j)} \end{array} \right] \quad [3]$$

where $C_b^{i,j} = \frac{h^3}{12} \frac{E_1}{1-\nu_1\nu_2}$.

The torsional energy, stored in the torsional spring $C_t^{i,j}$, is expresses as

$$U_{t(i,j)} = \frac{1}{2} C_t^{i,j} \left[\Delta\psi_{xy(i,j)}^2 \frac{\Delta x}{\Delta y} + \Delta\psi_{yx(i,j)}^2 \frac{\Delta y}{\Delta x} \right], \text{ where } C_t^{i,j} = G \frac{h^3}{6} \quad [4]$$

The strain energy U_s of the lattice is then the sum of the previous contributions, viz

$$U_s = \sum_{i=1}^{n} \sum_{j=1}^{m} U_{b(i,j)} + \sum_{i=1}^{n-1} \sum_{j=1}^{m-1} U_{t(i,j)} + \sum_{i=1}^{n} \sum_{j=1}^{m} U_{ex(i,j)} + \sum_{i=1}^{n-1} \sum_{j=1}^{m-1} U_{sh(i,j)} \quad [5]$$

where n and m are the total number of chains in the x and y directions (longitudinal and transversal) respectively.

The configuration shown in Figure 2 gives the kind of applied boundary conditions: rotational springs of constants $C_{edgeN1}, C_{edgeN2}, C_{edgeN3}, C_{edgeN4}$ represent the rigidity of the edge supports and extensional springs of constant $C_{foundation}$ represent the equivalent elastic foundation rigidity. We assume the springs' constant to be uniform for each edge, whereas the edges' rigidities $C_{edgeN1}, C_{edgeN2}, C_{edgeN3}, C_{edgeN4}$ may be different. This system allows the study of the deformation and buckling considering different types of boundary conditions (free, elastic or clamped edges) (Kikuchi *et al*., 2000) and also in the case of a fabric sheet with lateral elastic contacts, or lying on an elastic foundation (Silva *et al*., 1998). These additional parameters allow the representation of a great diversity of boundary conditions.

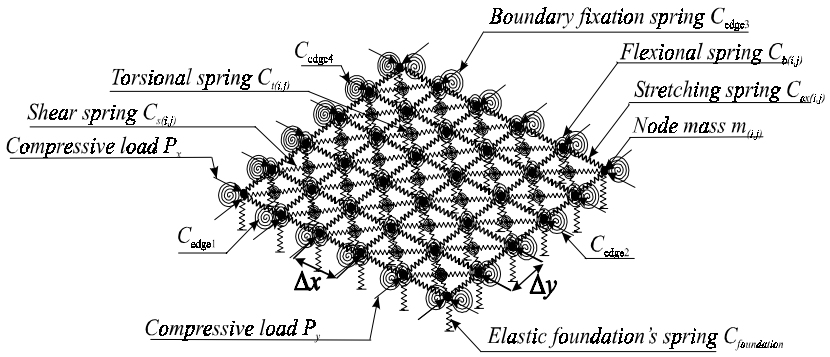

Figure 2. *Discrete fabric model resting on an elastic foundation with fixed edges*

The boundary conditions at the edges and the corners of the domain are the following:

– at the corner nodes, the bending stiffness is ignored (it is supposed nil, because there is no change in rotational angles);

– Considering the nodes of the longitudinal (resp. transversal) edges, we take only the longitudinal (resp. transversal) change in rotational angles $\Delta\psi_x$ (resp. $\Delta\psi_y$) into account, in order to express the bending strain energy stored in the rotational springs of these nodes.

We assume that the foundation extensional springs are connected to the grid nodes as shown in Figure 2. During fabric sheet deformation, the elongation of an extensional spring connected to a node labeled (i, j) is equal to $w_{(i,j)}$, thus, the total stretching energy of the foundation is:

$$U_{foundation} = \frac{1}{2}\sum_{i=1}^{n}\sum_{j=1}^{m} C_{foundation(i,j)} w_{i,j}^2 \qquad [6]$$

In order to take the rigidity of the edge's supports into account, it is assumed that at each boundary node, a rotational spring defined above is connected. The corresponding stored strain energy $U_{edge's\ fixation}$ can be written as

$$\begin{aligned} U_{edge'sfixation} = & \sum_{i=1}^{n} \frac{1}{2} C_{edgeN1} \psi_{y(i,1)}^2 + \sum_{j=1}^{m} \frac{1}{2} C_{edgeN2} \psi_{x(n-1,j)}^2 \\ & + \sum_{i=1}^{n} \frac{1}{2} C_{edgeN3} \psi_{y(i,m-1)}^2 + \sum_{j=1}^{m} \frac{1}{2} C_{edgeN4} \psi_{x(1,j)}^2 \end{aligned} \quad [7]$$

The total strain energy U of the discrete mechanical model is the sum

$$U = U_s + U_{edge's\ fixation} + U_{foundation} \quad [8]$$

The total potential energy of the structure is then the difference between the total strain energy and the external force's work, viz

$$V = U - W_{ext} \quad [9]$$

where W_{ext} is obtained by summing up the work of the gravitational forces and the work of the compressive loads P_x, P_y (discrete load): defining S the surface of the lattice, and ρ the mass density per unit area of the fabric, one obtains

$$\begin{aligned} W_{ext} = & -\rho g \frac{S}{n \times m} \sum_{i=1}^{n} \sum_{j=1}^{m} w_{i,j} + P_x \sum_{i=1}^{n-1} \sum_{j=1}^{m} \left[\Delta x (1 - \cos \psi_{x(i,j)}) - u_{(n,j)} \right] \\ & + P_y \sum_{i=1}^{n} \sum_{j=1}^{m-1} \left[\Delta y (1 - \cos \psi_{y(i,j)}) - v_{(i,m)} \right] \end{aligned} \quad [10]$$

with $P_x = p_x \Delta x$ and $P_y = p_y \Delta y$ the punctual nodal forces exerted in the x and y direction respectively. The two components p_x and p_y therein are the lineic densities of the uniform loads exerted in the plate directions x and y respectively.

The fabric is further assumed to undergo small stretching and shearing, provided it remains only submitted to its own weight and to small loads. We notice that the total potential energy involves two dependent variables ψ and *w*, where

$$\sin \psi_{x(i,j)} = \frac{w_{i+1,j} - w_{i,j}}{\Delta x}, \quad (i, j) \in [1, n-1] \times [1, m] \quad [11]$$

$$\sin \psi_{y(i,j)} = \frac{w_{i,j+1} - w_{i,j}}{\Delta y}, \quad (i, j) \in [1, n] \times [1, m-1] \quad [12]$$

These relationships remain valid for small deformations $\left(\Delta u_{(i,j)} << \Delta x \text{ and } \Delta v_{(i,j)} << \Delta y, \ \forall \ (i,j) \in [1..n;1..m]\right)$. Therefore it is possible to express *V* in terms of only three variables fields, either (u, v, ψ) or (u, v, w).

The fabric materials are assumed to be flexible structures, which undergo small stretching and shearing under their own weight or under low load value. Accordingly, in the sequel, we neglect the stretching and the shearing deformations. Therefore, using the previous assumption, the total potential energy will be expressed in terms of the sole displacement field w.

3. Draping simulations

We analyze the drape deformation of square fabric sheets draped over multi – geometrical surfaces or supported at p-fixed point positions, subjected to their own weight. Obviously, the geometry of surface supports, the position and the number of support points are important parameters. We shall focus to the case where the fabric sheet is placed upon a fixed rigid supporting body, which can represent a mold. The nodes in contact with the support surface or located on the support points, are fixed in all directions: this defines auxiliary conditions being treated here as an additional set of displacements constraints for the supported or draped fabric sheet, viz:

$$w_{k,l} = h_{(k,l)} \ ; \ (k,l) \in \Omega = \left\{(i,j) \in [1,n] \times [1,m], w_{i,j} = cst\right\} \qquad [13]$$

This constrained problem is solved by the classical method of Lagrange Multipliers (Bruckstein *et al*., 1990), whereby the following additional energy term U_{aux} is added to the potential energy of the structure:

$$U_{aux} = \sum_{(k,l)\in\Omega} \lambda_{(k,l)} \left(w_{k,l} - h_{(k,l)}\right) \qquad [14]$$

The Lagrange multipliers $\lambda_{i,j}$ are identified to the reaction forces of the fixed nodes of the trellis. At equilibrium, the first variation of the total potential energy $\tilde{V}$ must vanish, thus we the following system of equations shall be satisfied:

$$\frac{\partial \tilde{V}}{\partial w_{1,1}} = \frac{\partial \tilde{V}}{\partial w_{1,2}} = ... = \frac{\partial \tilde{V}}{\partial w_{i,j}} ..... = \frac{\partial \tilde{V}}{\partial w_{n,m}} = 0 \text{ and } \frac{\partial \tilde{V}}{\partial \lambda_{k,l}} = 0 \, , (k,l) \in \Omega \qquad [15]$$

An algorithm using the symbolic manipulation software Maple© has been written to generate and solve this system of algebraic equations. Note that in the case of large displacements, the system of equations is non-linear. The case of a continuous supporting surface is considered: the simulation of the draped shape of a piece of

fabric, a part of which is fixed on the surface of a square, subjected to its self-weight, has further been performed, (Figure 3), using the Maple© software.

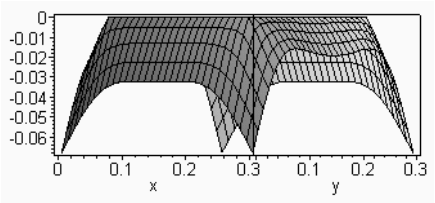

$E_1 = 175$ Kpa $E_2 = 120$ Kpa
$\nu_1 = 0.6$ $\nu_2 = 0.4$
$G = 33$ Kpa $h = 1.45$ mm
$\rho = 22$ g/m^2

Figure 3. *Draping of a square fabric sheet (31×31 nodes) posed over a square plate*

In a general case, the deformed shape of the draped fabric sheet is obviously dependent on the fabric properties (Yu. *et al* 2000) (bending stiffness, shear rigidity, Poisson's ratio, thickness and weight), the geometry of the support surface, the number and locations of the support points.

4. Stability analysis

Although many buckling plates (fabric sheet here) theories have been developed, engineers are still looking for some simple and useful models for general engineering problems (Timoshenko, 1947), (Nemeth, 1997), (Chai, 2002). Stability and buckling analysis for discrete beams may lead to original analyses with a simpler formulation, (Magno *et al.*, 2002). The stability analysis is used in order to determine the buckling load and corresponding mode shape for a given set of applied loads and constraints. Buckling behavior for fabric sheets plays an important role (formation of plies within the fabric). The fabric shape at equilibrium depends upon the boundary conditions, which take into account stitches, seams, lining, hem, pleat (local rigidity).

Stability is satisfied when the total potential energy V has a relative minimum at the equilibrium position, thus one looks for the minimum of the multivariable function $V(w_{1,1},..,w_{1,j},..,w_{1,m},..,w_{i,1},..,w_{n,m})$. The buckling analysis relies on the Dirichlet-Lagrange stability criterion (El Naschie, 1990), which involves the vanishing of a stability determinant, that determines the critical load. The stability matrix K is defined as the Hessian matrix of the total potential energy function V of the mechanical structure, viz

$$K_{i,j} = \left(\frac{\partial^2 V}{\partial \mathbf{w} \partial \mathbf{w}} \right)_{i,j}, \text{ with } (i,j) \in [1..n \times m; 1..n \times m] \qquad [16]$$

The critical state of stability shall then be detected from the condition

$$\mathrm{Det}(K) = 0 \qquad [17]$$

Only the first root value of equation [17] or the lowest bifurcation point is interesting, indicating that the state of equilibrium changes from stable to unstable: this change marks the occurrence of the buckling load. The state of equilibrium is stable if and only if the stability determinant $\mathrm{Det}(K)$ and its principle minors $\mathrm{Det}\left(K_i\right)_i$ are all positive (in the opposite case, the equilibrium will be unstable). The number of stability roots is an indication about the corresponding number of passed bifurcation points. In order to illustrate the application of the Dirichlet-Lagrange criterion, we consider a square fabric sheet simply supported at all four edges and uniformly compressed in the x-direction only (Figure 4).

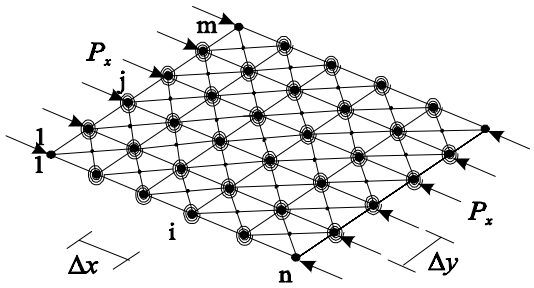

Figure 4. *Square fabric simply supported at its edges compressed in the x-direction*

The square fabric sheet is discretized in a truss of n longitudinal chains and m transversal chains. We restrict to the case where m is equal to n *(i.e.* $\Delta x = \Delta y = \Delta$). In this example, we suppose that the fabric sheet has the same properties in the x and y directions, thus behaves as an isotropic plane material. This implies

$$E_1 = E_2 = E \text{ and } \nu_1 = \nu_2 = \nu \qquad [18]$$

Denoting by $D = \frac{E}{1-\nu^2}\frac{h^3}{12}$ the bending rigidity and by $T = G\frac{h^3}{6} = D(1-\nu)$ the torsional rigidity of the fabric sheet.

Differentiating V with respect $w_{1,1},..,w_{1,j},..,w_{1,m},..,w_{i,1},..,w_{n,m}$, the stability matrix S of a square lattice of 12 elements bars is expressed in term of $\lambda := \frac{P\Delta}{D}$.

The smallest root, of the equation $\det(S) = 0$, is $\lambda = 0.4824$ which corresponds to the approximate critical load gives

$$p_x^c = \frac{P_x^c}{\Delta} = \frac{\lambda D}{\Delta^2} = 3.977\frac{D}{L^2} \qquad [19]$$

The exact solution of the same buckling problem is (Kapur, 1996).

$$P^{c}_{exact} = 4\frac{\pi^2 D}{L^2} \qquad [20]$$

The comparison of the values given in (Chai, 2002), (El Naschie, 1990) – the error in the critical load is about 0.5% – demonstrates the good accuracy of the present model. Compared to other methods (Rayleigh-Ritz method, finite differences or finite elements), the stability analysis conduced on the basis of the discrete model proves simpler to handle (El Naschie, 1990), since the form of the criterion itself receives a simpler expression, and it further proves convenient for the study of the effect of a wide range of configuration parameters, such as the effect of structure orthotropy, structure size and boundary conditions.

5. Mesoscopic model

As previously mentioned, the analysis of the motion and behaviour of the dry fabric (before it is being impregnated with a resin, such as in the RTM process) is very peculiar, due to the relative easy of motion of the yarns. This motion in turns determines the shape forming of the woven structure, thus calls for a separate analysis (Kawabata *et al*., 1973), (Gasser *et al*., 2000). As the woven structure becomes stretched, the interaction between both sets of yarns (warp and weft) is mobilized, and one should expect that the ability of the tissue to deform shall be accordingly hindered (due to a change of deformation mechanisms): it is intuitively clear that the yarn mobility is reduced at the contact zone between both yarns, specially in terms of rotation. This in turn affect the shape forming capacity of woven structures at the macroscopic scale. Few works in the literature have been devoted to the analysis of the interactions between the yarns, notwithstanding 3D finite element analysis within a context of contact mechanics (Page and Wang, 2002). The goal of the mesoscopic approach is to incorporate the effect of the yarn interactions, without considering the three-dimensional picture inherent to a microscopic view of the yarns contact problem. For that purpose, a more refined analysis of the yarn motion is performed, whereby the yarns undulations are explicitly considered: for that reason, it is given the coinage mesoscopic modeling, see (Ben Boubaker *et al*., 2003).

5.1. *Single yarn motion accounting for transverse yarns reactions*

In order to exemplify the methodology, one considers in the sequel the plane motion of a single yarn (the warp, here labeled Y^{k}_{wa} for the k^{th} yarn) that we mentally isolate from the woven structure, subjected to a traction effort at its extremities and to the punctual contact reactions exerted by the transverse yarns (the weft), see the left side of Figure 5.

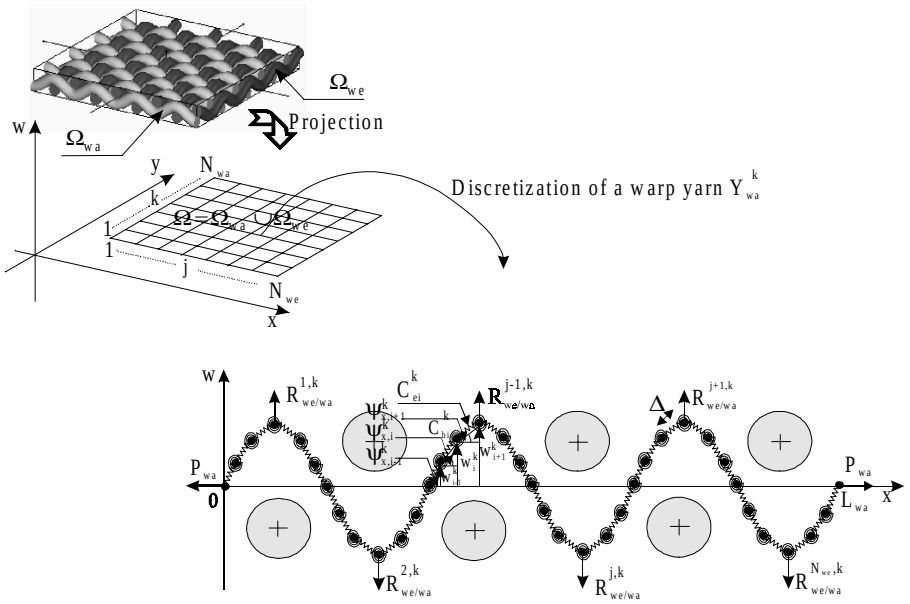

Figure 5. *Discrete model of the yarn isolated from the trellis*

Although this situation is somewhat artificial (since we isolate mentally the yarn from the trellis), it gives a first insight into the coupling effect between both sets of yarns. The discretized yarn consists of a set of punctual masses mutually connected by extensional rigidities $C_{ei} = EA/\Delta$; each node is given a rigidity in flexion $C_{bi} = EI/\Delta$ (Δ is the curvilinear distance between two consecutive nodes), Figure 5. Compared to the trellis model which neglected the extension of the yarns, the discrete elements of the undulated yarn are here endowed with an additional extension mode.

5.2. *Weft and warp force interactions in the case of a biaxial loading of the fabric*

These expressions at hand, the extension of this analysis for the whole network is straightforward and is just a matter of having a double indexing system for the nodes of the network (the first index being attached to the warp and the second to the weft). At equilibrium, the deformed shapes of the fabric yarns are assumed to be periodic and accordingly expressed as the following Fourier series:

– $w_{we}^{j}(y) = \sum_{n=1}^{N_{wa}} a_{n,j}^{we} \sin\left((j-1)\pi + n\frac{\pi y}{L_{we}}\right)$, for a weft yarn of index j

– $w_{wa}^{k}(x) = \sum_{n=1}^{N_{we}} a_{n,k}^{wa} \sin\left((k-1)\pi + n\frac{\pi x}{L_{wa}}\right)$, for a warp yarn of index k

The set of intertwined yarns Ω is decomposed into the assembly of two sub mechanical systems (Figure 5) namely the set of warp yarns, Ω_{wa}, being in interaction with the set of weft Ω_{we}, here considered as an external (sub-mechanical) system.

In order to establish the expression of the reaction force exerted at the yarn-yarn contact points, we analyze the mechanical behavior of the system Ω_{we} consisting of the N_{we} weft yarns: since the sub-system Ω_{wa} consisting of the set of warp (N_{wa} yarns) is considered as an external system, the contact forces exerted on the weft yarns are considered as external forces for Ω_{we}. Using the Timoshenko's beam theory, in the case of an elastic beam subjected to an axial load P and a lateral force F exerted at a point of abscissa c (Figure 6), the equilibrium shape of the elastic beam is given by the Fourier series

$$w(x) = \frac{2FL^3}{\pi^4 EI} \sum_{k=1}^{N} \frac{1}{k^2\left(k^2 + \frac{P}{P_{cr}}\right)} \sin\left(\frac{k\pi c}{L}\right) \sin\left(\frac{k\pi x}{L}\right) \qquad [21]$$

with, $P_{cr} = \frac{\pi^2 EI}{L^2}$, the beam critical compressive load for buckling, L the projected beam length and EI the beam bending rigidity.

Figure 6. *Elastic beam subjected to lateral and axial loads*

Using the superposition principle, the equilibrium shape associated to a weft yarn of index j, treated as an elastic beam subjected to an axial load and periodic lateral forces, is defined in terms of the reaction force $R_{wa/we}$, as, viz

$$w_{we}^{j}(y) = \frac{2R_{wa/we}L_{we}^3}{\pi^4 EI_{we}} \sum_{n=1}^{N_{wa}} \sum_{m=1}^{N_{wa}/2} \frac{1}{n^2\left(n^2 + \alpha_{we}\right)} \left(\begin{array}{l} \sin\left(\frac{n\pi}{N_{wa}}\left(2m - \frac{3}{2}\right)\right) \\ -\sin\left(\left(2m - \frac{1}{2}\right)\frac{n\pi}{N_{wa}}\right) \end{array} \right) \sin\left((j-1)\pi + \frac{n\pi y}{L_{we}}\right) \qquad [22]$$

with $\alpha_{we} = \frac{P_{we}}{P_{cr}^{we}}$, and $P_{cr}^{we} = \frac{\pi^2 EI_{we}}{L_{we}^2}$ the critical weft compressive buckling load.

This result shows that the deformed shape of the weft yarns within a woven structure at equilibrium is known from the values of the applied traction P_{we} (trough the ratio α_{we}) and the yarn-yarn contact forces. We note $\tilde{w}_{we} = A_{we}$ the amplitude of the weft yarns within the woven structure, defined at the contact points abscissas (Figure 7) by $y = c_k$, $\tilde{w}_{we} = \left| w_{we}^{j}(y) \right|$

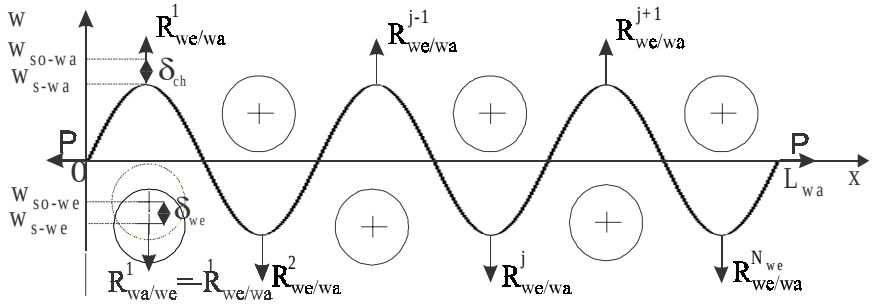

Figure 7. *Motion of the undulated warp: kinematic variables and reaction forces*

At the interlacing points ($y = c_k$, $\forall k \in [1, N_{wa}]$), the new double sum of the Equation [22] renders after a tedious but elementary calculation

$$\left| \sum_{n=1}^{N_{wa}} \sum_{m=1}^{N_{wa}/2} \frac{1}{n^2\left(n^2+\alpha_{we}\right)} \begin{pmatrix} \sin\left(\frac{n\pi}{N_{wa}}\left(2m-\frac{3}{2}\right)\right) \\ -\sin\left(\left(2m-\frac{1}{2}\right)\frac{n\pi}{N_{wa}}\right) \end{pmatrix} \sin\left((j-1)\pi + \frac{n\pi y}{L_{we}}\right) \right| = \frac{1}{N_{wa}\left(N_{wa}^2+\alpha_{we}\right)} \quad [23]$$

We then deduce, from Equation[22], the expression of the reaction forces exerted by the transverse yarns on the weft yarns at the interlacing points: the amplitude undulations have the value $\tilde{w}_{we} = A_{we}$, thus we obtain

$$y = c_k, \quad \left|w_{we}(y)\right| = \tilde{w}_{we} = \frac{2R_{wa/we}}{\pi^4 EI_{we}} \frac{L_{we}^3}{N_{wa}\left(N_{wa}^2 + \alpha_{we}\right)}$$
$$\Leftrightarrow R_{wa/we} = \frac{\pi^4}{2} \frac{EI_{we}}{\left(L_p^{we}\right)^3} \left(1 + \frac{\alpha_{we}}{N_{wa}^2}\right) \tilde{w}_{we} \qquad [24]$$

In the specific case of only one reaction force ($N_{wa} = 1$) applied at the middle of the yarn, we find a result identical to that of (Timoshenko, 1947), viz

$$F = \frac{\pi^4}{2} \frac{EI}{L^3} (1 + \alpha)\ \tilde{w} \qquad [25]$$

5.3. *Effect of the yarn interactions on the traction behavior*

Under the effect of the loads P_{wa} and P_{we} applied respectively in the warp and weft directions (supposed to be uniformly distributed along the edge nodes), an undulation transfer due to the yarn-yarn interaction occurs at the contact points ; this undulation transfer process is followed by a lateral displacement of the contact points (Figure 11). The displacement continuity occurring at the crossing points labeled by the set of indices (j,k) then expresses as

$$w_{s-we}^{j,k} = w_{so-we}^{j,k} + w_{s-wa}^{j,k} - w_{so-wa}^{j,k} \qquad [26]$$

where j is the index of the weft yarn and k the index of the warp yarn. This relation can further be interpreted in purely geometrical terms as an undulation transfer between the two mechanical systems Ω_{wa} and Ω_{we}: when the undulation decreases in one direction, an increase in the transverse direction of the transverse yarn occurs (Figure 7). From the relations [24] and [26], we get

$$R_{wa/we}^{j,k} = \frac{\pi^4}{2} \frac{(EI)_{we}}{\left(L_p^{we}\right)^3} \left(1 + \frac{\alpha_{we}}{N_{wa}^2}\right) \left[(w_{so-we}^{j,k} - w_{so-wa}^{j,k}) + w_{s-wa}^{j,k} \right] \qquad [27]$$

The action-reaction principle, $R_{we/wa}^{j,k} = -R_{wa/we}^{j,k}$, further gives

$$R_{we/wa}^{j,k} = -\frac{\pi^4}{2} \frac{(EI)_{we}}{\left(L_p^{we}\right)^3} \left(1 + \frac{\alpha_{we}}{N_{we}^2}\right) \left[(w_{so-we}^{j,k} - w_{so-wa}^{j,k}) + w_{s-wa}^{j,k} \right] \qquad [28]$$

The work of the reaction force exerted by a weft yarn of index j on the warp yarn of index k, occurring at the interlacing point (j,k), is then evaluated as

$$W_{R^{j,k}_{we/wa}} = -\frac{\pi^4}{2}\frac{(EI)_{we}}{\left(L_p^{we}\right)^3}\left(1+\frac{\alpha_{we}}{N_{wa}^2}\right) \left[\begin{array}{l}\left((w^{j,k}_{so-we} - w^{j,k}_{so-wa})w^{j,k}_{s-wa} + \frac{1}{2}w^{j,k\ 2}_{s-wa}\right) \\ -\left((w^{j,k}_{so-we} - w^{j,k}_{so-wa})w^{j,k}_{so-wa} + \frac{1}{2}w^{j,k\ 2}_{so-wa}\right)\end{array}\right] \quad [29]$$

This expression shows the influence of the transversal yarns characteristics EI_{we}, L_p^{we}, $w_{so\text{-}we}$, $w_{s\text{-}we}$ and of the coefficient $\alpha_{we} = \frac{P_{we}}{P_{cr}^{we}}$ - which quantifies the interaction between the two sub-mechanical systems Ω_{wa} and Ω_{we} - during the loading - on the work of the reaction force exerted on the warp yarn. Accordingly, the total work of the reaction forces exerted on a warp yarn of index k is the sum

$$W^k_{\text{reaction forces}} = \sum_{j=1}^{N_{we}} W_{R^{j,k}_{we/wa}}$$

The total potential energy V becomes a function of the Fourier coefficients $\left(a^{wa}_{p,k}\right)_{(p,k)\in[1..N_{we};\ 1..N_{wa}]}$ and of the yarn nodal extensions $\left(u^k_2, u^k_3, ..., u^k_{N_d+1}\right)_{k\in[1..N_{wa}]}$, viz

$$V = V\left(a^{wa}_{1,k}, ...a^{wa}_{i,k}, ..., a^{wa}_{N_{tr},k}, u^k_2, ...u^k_i, ...u^k_{N_{d+1}}\right)_{k\in[1..N_{wa}]} \quad [30]$$

We assume that the woven structure is fixed at the side $x = 0$, thus the condition

$$\left(u^k_1 = 0\right)_{k\in[1..N_{wa}]} \quad [31]$$

The equilibrium state of the sub-mechanical system Ω_{wa} is characterized by the minimum of the total potential energy V ; thereby, the first variations of the total potential energy vanish, leading to the following system of algebraic equations:

$$\left(\frac{\partial V}{\partial a^{wa}_{i,k}}\right)_{(i,k)\in[1..N_{we};\ 1..N_{wa}]} = 0 \quad \text{and} \quad \left(\frac{\partial V}{\partial u^k_i}\right)_{(i,k)\in[2..N_{d+1},1..N_{wa}]} = 0 \quad [32]$$

Considering carbon fibers reinforced fabric, the following input parameters are used (SNECMA, 2002): the mechanical properties of the warp and weft yarns are taken as:

$$\begin{cases} EI_{wa} = 1.47e^{-7}\,\text{N.m} \\ EI_{we} = 1.47e^{-7}\,\text{N.m} \\ EA_{wa} = 13.72\ \text{N} \end{cases}$$, The rigidities in flexion/extension of the springs are then evaluated as $C_b = \frac{EI_{wa}}{\Delta}$; $C_e = \frac{EA_{wa}}{\Delta}$. The geometrical parameters of the discretization scheme are: $\begin{cases} L_0 = 0.1\text{m} & N_{we} = 16\ ;\ N_d = 224 \\ w_{so-wa} = 0.5\text{mm} & w_{so-we} = 0.5\text{mm} \end{cases}$

The mean curve of the yarn is restricted to the (x, y) plane, (Figure 7), and both extremities of the yarn keep aligned with the direction of traction. The extension of the yarn is here defined as the displacement of the end node of the undulated beam. The yarn is subjected to an increasing traction at its extremities, and one represents the traction load vs. the yarn end-displacement (Figure8) ; the simulation without yarn interactions serves as a reference comparison case to assess the interaction effect.

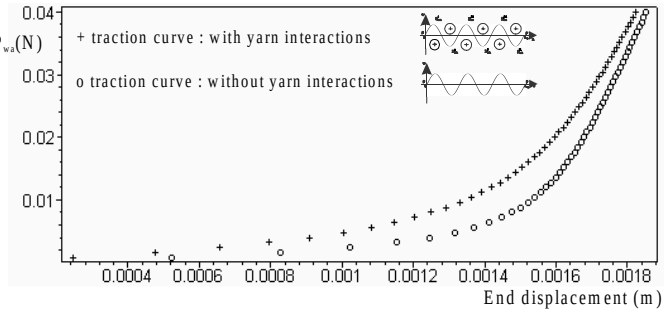

Figure 8. *Unidirectional traction curve of the warp yarn. Effect of yarn-yarn interactions*

The obtained J-shape (Figure 8) of the fabric tensile response is in good agreement with observed experimental results (Boisse, 1997). The consideration of the yarn-yarn interactions leads to a stiffer response of the yarn (Figure 8): during traction, the transverse yarns resist the yarn-yarn undulation transfer by increasing the reaction force. This explains why, without considering yarn-yarn interactions, the loss of undulations is more rapid, compared to the case with yarn-yarn interactions. We can distinguish two nearly linear parts: the first part (up to an applied force of about 0.01 N) is due to the yarn-yarn undulation transfer, which traduces a decrease of the warp undulation. At the end of the transfer of undulation (the structure is

nearly blocked regarding the variations of undulation), a stiffer response represented by the non-linear part is obtained, due mostly to the extension of the yarn. During the fabric deformation process, the end nodes (located at the free edge) undergo an axial displacement, due to a flexional contribution (variation of the undulation) and an extensional contribution (displacement due to the fabric stretching).

The deformation mechanisms of the fabric, viz the change of yarn undulation and the yarn stretching are next analyzed. The global displacement Δu_{wa} experienced by the end nodes of the warp is obtained as the sum of a flexional displacement contribution Δu_{wa}^{f} (yarn end-displacement due to the undulation variation) and the extensional displacement contribution Δu_{wa}^{ex} (yarn end-displacement due to the stretching of the yarn), with

$$\Delta u_{wa}^{f} = \sum_{i=1}^{N_d} \Delta\left(\cos\left(\psi_{x,i}\right) - \cos\left(\psi_{x,oi}\right)\right) \text{ and } \Delta u_{wa}^{ex} = \sum_{i=1}^{N_d} \Delta u_i = u_{N_d+1} \qquad [33a,b]$$

Accordingly, one has the following additive decomposition of the total displacement

$$\Delta u_{wa} = \sum_{i=1}^{N_d} \Delta\left(\cos\left(\psi_{x,i}\right) - \cos\left(\psi_{x,oi}\right)\right) + u_{N_d+1} \qquad [34]$$

The separate variations of the flexional and the extensional displacements are illustrated in Figure 9, using equation [33a,b]; the transverse load is here assigned a nil value (thus $P_{we} = 0.0 P_{wa}$).

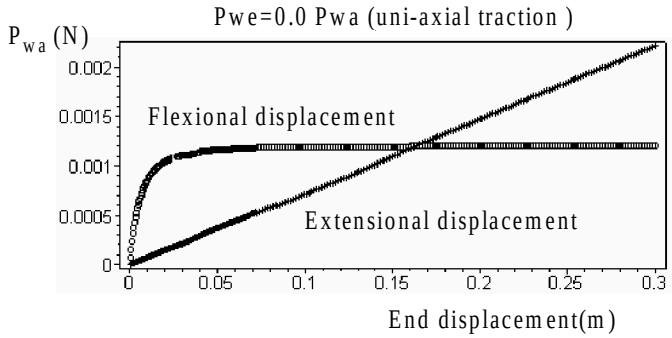

Figure 9. *Flexional and extensional displacements variations vs. the applied load (case of uniaxial load)*

The flexional displacement tends toward a limit value, which indicates that the yarn has exhausted it variation of undulations, whereas the extensional displacement

linearly varies vs. the applied load, which shows that this deformation mechanism is not influenced by the change of yarn undulations.

5.4. *Fabric under uni-axial extension: effect of yarns mechanical properties*

The reaction load at the interlacing points depends on the weft mechanical parameter, as evidenced by equation [28]. In order to asses the effect of the mechanical and geometrical characteristics on the fabric traction behavior, simulations of the traction behavior of the fabric in the warp direction are performed for different values of the transverse yarns rigidity. Figure 10 shows that a stiffer transverse yarn increases the reaction forces, thus leads to a stiffer response of the warp (Figure 11).

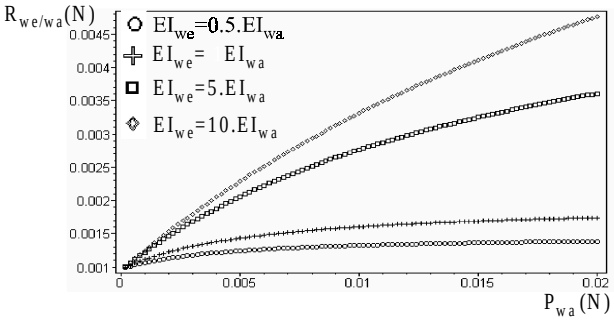

Figure 10. *Variation of the reaction force. Effect of warp and weft modulus*

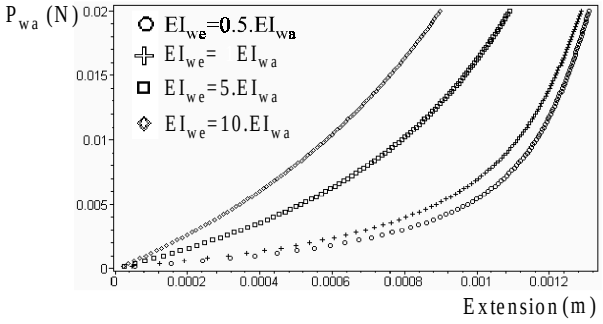

Figure 11. *Fabric extension in the warp direction. Effect of the weft modulus*

At the end of this stiffening, the reaction force tends toward a limit value, which indicates that the yarn has exhausted its possibilities of undulation changes.

5.5. *Fabric under bi-axial extension*

We analyze the effect of the transverse extension load P_{we} on the fabric mechanical behavior, in the warp direction (x-direction). We can deduce from Equation [28] that the reaction force occurring at the interlacing points varies with P_{we}, thus leads to different fabric traction responses. The followings values of the extension load P_{we} are considered (viewed here as a parameter):

$P_{we} \in \{0.0\ P_{wa}, 0.1\ P_{wa}, 0.2\ P_{wa}, 0.3\ P_{wa}\}$.

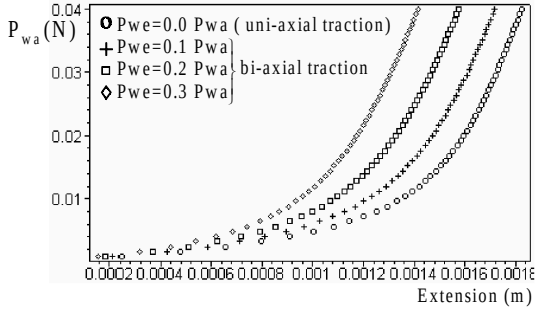

Figure 12. *Fabric traction curves: effect of the transverse extension load* P_{we}

The results (Figure 12) show that increasing the transverse extension load P_{we} leads to a stiffer response of the fabric: this is due to the decrease of the yarn-yarn undulation transfer capacity. Indeed, from Equation [28], we remark that as P_{we} increases, the reaction load $R_{we/wa}$ increases, which affects the yarn-yarn undulation transfer, thus leading to a stiffer response. We further record the variation of the reaction load $R_{we/wa}$, occurring at the crossing points, vs. the applied extension load P_{wa} (in the x-direction), considering different values of P_{we} (given in [28]), Figure 13.

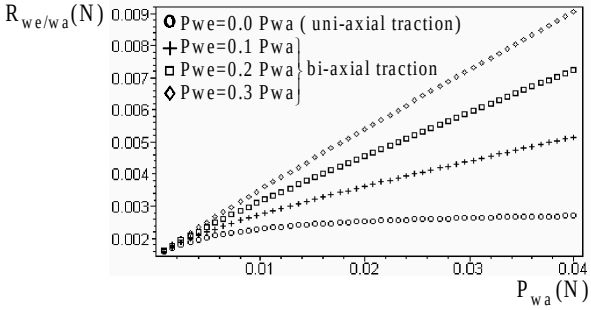

Figure 13. *Variation of the reaction load* $R_{we/wa}$ *: effect of the transverse load* P_{we}

The reaction force $R_{we/wa}$ increases with the transverse extension load P_{we}. Although the reaction load $R_{we/wa}$ tends toward a limit value in the case of an uni-axial extension ($P_{we} = 0$), we remark that, in the case of biaxial extension, it grows continuously without reaching a limit value: Equation [28] shows that the reaction force $R_{we/wa}$ not only varies according to the position of the warp/weft yarns' summits, but also according to the transverse extension load P_{we}. In fact, when the yarn-yarn undulation transfer process is exhausted, the reaction force does not vary any more (since the positions of the contact points between yarns do not change any more) ; it solely varies vs. P_{we}, with a linear variation that explains the linear part observed on the biaxial traction curves.

6. Conclusion

A discrete mass-spring model of the mechanical behavior of a woven fabric sheet, built from the repetition of a basic unit cell made of four beams connected by rotational rigidities, and two torsional springs along the diagonals. The kinematics of the discrete unit cell combines stretching and shearing in plane deformations with flexional and torsional deformation modes. Discrete models present the advantage that the basic constituent of the trellis, the yarn, is explicitly modeled, thus the developed models have a predictive nature ; they are thought to bring a help for the design of specific fabric, since they allow to analyze the influence of several geometrical and mechanical parameters (mechanical properties and organization of the yarns within the unit cell). Such micromechanical analyses shall be extended towards consideration of more complex armors (serge, satin, 3D weaving).

We have next developed a refined discrete mass-spring model of a woven structure at a mesoscopic level, whereby the yarn undulations and the yarn-yarn interactions are taken into account. The simulated macroscopic behavior of the fabric appears strongly depends on the mechanical and geometrical yarns parameters and also on the ratio of the biaxial loading. The contribution to the total deformation of the flexional displacement (due to the undulations variation) and of the extensional displacement (due to the yarns stretching) has been analysed.

Although expensive from computational point of view when dealing with large scale analysis (structural analysis), the discrete models prove convenient when important changes of curvature occur, since the microstructure (yarn intertwining) plays there an important role. Clearly, the discrete modelling approach shall prove simpler to implement compared to the continuous strategy in the case of more complex armors (such as serge, satin, or even three-dimensional weaving). Further work remains to be done in this direction.

The consideration of the yarns compressibility and the friction between yarns constitutes one of the main perspective of development of the discrete modeling strategies of fabric.

7. References

B. Ben Boubaker, B. Haussy, J.F. Ganghoffer, "Discrete models of woven structures ; Draping and stability analysis", *CRAS, Série Mécanique*, n° 330, 2002, p. 871-877.

B. Ben Boubaker, B. Haussy, J.F. Ganghoffer, "A discrete model for the coupling between yarns in a woven fabric", *CRAS, Série Mécanique*, n° 331, Issue 4, 2003, p. 295-302.

B. Ben Boubaker, Mise en œuvre de modèles discrets du comportement mécanique de structures tissées, PhD thesis, INPL (Nancy), 2004.

Boisse P., Borr M., Buet K., Cherouat A., "Finite element simulations of textile composite forming including the biaxial fabric behaviour", *Composites*, Part B 28B, 1997, p. 453-464.

Boisse P., Daniel J.L., Gasser A. , Hivet G., Soulat D., « Prise en compte du procédé de fabrication dans la conception des structures composites minces », *Mec. Ind.*, n° 1, 2001, p. 303-311.

Bruckstein A.M., Netravali A.N., "On Minimal Energy Trajectories", *Computer Vision, Graphics and Image Processing*, n° 49, 1990, p. 283-296.

El Naschie M.S., *Stress-Stability and Chaos in Structural Engineering: an Energy Approach*, London: McGraw-Hill, 1990.

Ganghoffer J.F., "New concepts in nonlocal continuum mechanics and new materials obeying a generalised continuum behaviour",. *Int. J. Engng Sci.*, vol. 41, Issues 3-5, March 2003, p. 291-304.

Gasser A., Boisse P., Hanklar S., "Mechanical behaviour of dry fabric reinforcements. 3D simulations versus biaxial tests", *Computational Materials Science*, vol. 17, 2000, p. 7-20.

Hing H., Grimsdale R.L, "Computer graphics techniques for modeling cloth", *IEEE Computer Graphics and Applications*, vol. 16, n° 5, 1996, p. 28-41.

Kapur K.K., Billy J., Asce M., "Stability of Plates Using the Finite Element Method", *Journal of Engineering of Mechanics*, Division (EM2), 1996, p. 77-195.

Kawabata S., Niwa M., Kawai H., *Journal of the Textile Institute*, vol. 64, n° 21,1973.

Kawabata S., "Nonlinear mechanics of woven and knitted materials", *Textile Structural Composites*, vol. 3, 1989, Amsterdam, Elsevier, p. 67-116.

Kikuchi F., Ishii K., "Unification of Kirchhoff and Reissner-Mindlin Plate Bending Elements", European Congress on Computational Methods in Applied Sciences and Engineering, *ECCOMAS 2000*, Barcelona, 2001, 1-14 September.

Magno M., Lutz R; "Discrete buckling model for corrugated beam", *Eur. J. Mech. A/ Solids*, vol. 21, 2002, p. 669-682.

Magno M., Ganghoffer J.F., Postle R., Lallam A., "A mesoscopic wave model for textile materials in large deformations", *Composites structures*, vol. 57, 2002, p. 367-371.

Nemeth M.P., "Buckling Behavior of Long Symmetrically Laminated Plates Subjected to Shear and Linearly Varying Axial Edge Loads", Nasa TP-3659, July 1997.

Page J., Wang J., "Prediction of shear force using 3D non-linear FEM analyses for a plain weave carbon fabric in a bias extension state", *FEAD*, 38 (8),p. 755-764, 2002.

Provot X., "Deformation constraints in a mass-spring model to describe rigid cloth behavior", *Graphics Interface*, 1995, p. 147-155.

Realf M.L, Boyce M.C., Backer S., "A micromechanical approach to modelling tensile behaviour of woven fabrics", V.J. Stokes (Ed.), *Use of Plastic and Plastic Composites: Material and Mechanics Issue*, vol. 46, 1993, ASME, New York, p. 285-293.

Silva A.R.D. *et al*., "Analysis of Plate Under Contact Constraints", *Computational Mechanics New trends and Applications*, 1998, CIMNE, Barcelona.

SNECMA Moteurs, Le Haillan, France, Internal Report, 2002.

Timoshenko S., *Théorie de la Stabilité Elastique*, Paris & Liège, Beranger, 1947.

Tollenaere H., Caillerie, D., « Continuous modeling of lattice structures by homogenization », *Advances in Engineering Software*, n° 7-9, 1998, p. 699-705.

Yu W.R., Kang T.J., Chung K., "Drape Simulation of Woven Cloth Using Explicit Dynamic Analysis", *Journal of the Textile Institute*, vol. 91, 2000, Part I n°.2, p. 285-301.